



Optimisation of Subwoofer Placement using a Finite-Difference Time-Domain Acoustic Simulation

Delano Flipse

Supervisors: Prof. Dr. Elmar Eisemann, Dr. Jorge Martinez Castaneda

¹EEMCS, Delft University of Technology, The Netherlands

A Thesis Submitted to EEMCS Faculty Delft University of Technology,
In Partial Fulfilment of the Requirements
For the Bachelor of Computer Science and Engineering
January 29, 2023

Name of the student: Delano Flipse

Final project course: CSE3000 Research Project

Thesis committee: Prof. Dr. Elmar Eisemann, Dr. Jorge Martinez Castaneda, Prof. Dr. Marcus Specht

An electronic version of this thesis is available at <http://repository.tudelft.nl/>.

Abstract

The placement of a subwoofer has significant impact on the quality of its sound reproduction. This paper presents a method to optimise subwoofer placement in a room. Resonances caused by room boundaries (called “room modes”) cause localised peaks and lows for specific lower frequencies. The goal is to minimize the simulated frequency response over a listener region. To simulate the frequency response of a subwoofer location, a Finite-Difference Time-Domain method is applied. The results show that this method correlates to both a measured frequency response and an analytical model. The optimal location predicted with the simulation could not flatten every room mode, but had decreased variation for a number of resonant frequencies.

1 Introduction

Perfect sound reproduction is the holy grail of high quality audio enthusiasts. After a century of developing methods to perfect sound reproduction, it still remains an unresolved puzzle. One part of this broad and interconnected challenge is perfecting sound reproduction at the lower frequencies, where sound is produced by the subwoofer of the sound system.

The placement of a subwoofer has a significant influence on the low frequency acoustic performance of a room [1], [2]. At these frequencies, the quality of sound reproduction is dominated by wave interactions such as resonance and diffraction. Sound waves of the frequencies 20hz and 200hz, the range covered by most subwoofers, have a wavelength of 17m and 1.7m respectively. When a wavelength correlates to a room’s dimensions, resonances called “room modes” occur that cause significant positional peaks and lows in the “response” for that frequency. As a result, there is a large variation in the frequency response for a subwoofer. Placing a subwoofer at the right position can minimise this effect. However, predicting a good location is complicated by the effect of diffraction: the phenomena where sound bends around corners and objects. This effect is considerable for lower wavelengths. The complex interference pattern caused by reflections and diffraction makes it challenging to locate an optimal placement for the subwoofer with minimal frequency response variation.

To do so, mathematical analyses have been performed on the effect of boundaries (walls) on sound reproduction. Early studies have investigated the effect of nearby reflecting boundaries[3]. Later, this was extended to the effect of all boundaries, and models were created for rectangular rooms[4], [5]. More recently, methods for utilizing multiple subwoofers to treat room modes have been devised[1], [2].

Parallel to developing analytical models for subwoofer positioning, efforts have been made to accurately simulate sound as a wave. For the approximation of sound on a computer, multiple methods have been developed. One of the simplest methods to simulate how sound behaves over time is

the Finite-Difference Time-Domain (FDTD) method. This method has been applied to simulate low-frequency room acoustic problems for some time[6], [7]. As a result, the spectral, directional and qualitative properties of this method have been analysed to great extent [8], [9]. Additionally, with the increase in computing power, this method has become a viable option to simulate sound in reasonable time for lower frequencies[10]. In the context of optimizing the location of sound sources, the FDTD method has been employed to minimise noise experienced at the listener regions [11].

However, the analytical models only account for room modes caused by the outer walls of the room, and only for rooms with a rectangular shape. As a result, these models do not suffice for rooms with different shapes, or with large objects in them. As for the FDTD method, efforts have proven that the method is able to simulate sound with a high correlation to real measurements[12]. However, up until our current knowledge, this method is yet to be applied to finding optimal subwoofer positioning for minimal frequency response variation as a measure.

The aim of this work is to find a simulated optimal location for a subwoofer with a minimal frequency response variation in a room using the FDTD simulation method. Using this method, all possible subwoofer positions are evaluated, and for each, the average variation in frequency response is determined for the listener regions. When doing so, an optimal position was found based on the minimal variation. The duration of the process is speed up using a GPU-accelerated implementation. The results show that this method can simulate sound with some correlation to reality, and can find an location with less variation in frequency response.

Necessary background information about the topic of sound simulation is given in Section 2. The used methodology is described in Section 3. In Section 4, the results are presented. Section 5 reflects on the ethical implications and considerations of this research. Results, and potential future work is discussed in Section 6. Finally, a conclusion is given in Section 7.

2 Background

2.1 Acoustic Simulation Methods

Acoustic simulations are classified into two main categories: geometrical and wave-based. Geometrical Acoustic (GA) methods approximate sound as a particle or ray. In wave-based simulations, the acoustic wave equation is discretely solved for (a subdivision of) the simulated space.

Both have their advantages and disadvantages. GA simulations achieve great performance and are accurate for higher frequency, where wave phenomena are less prevalent[13]. However, at lower frequencies this method becomes unreliable[14]. This is due to wave phenomena such as diffraction and room mode interference becoming more pronounced, which a GA does not inherently simulate. Only at great cost, or reduced accuracy, can a GA simulation approximate these wave phenomena[14].

Wave simulations are computationally expensive, requiring both memory usage and computational power increase to accurately simulate higher frequencies and/or larger volume

spaces. This approach does provide an accurate representation of the whole sound field in a room, and can account for complex acoustic phenomena.

Additionally, there are hybrid simulations[15], which perform both types of simulation in parallel simulations, within their appropriate frequency ranges, with a defined crossover.

Wave-based simulations can be subdivided into frequency- and time-domain simulation methods. Although the frequency domain is better for steady-state problems, the time-domain is more intuitive (given the similarity with sound in reality) and the math less complex. It also allows for investigating time-domain properties like decay and reverberation.

For the purpose of this work, an implementation of a time-domain simulation using the finite-difference method was chosen since it is able to provide a simple implementation which is highly parallelizable (as described in Section 2.6). Although this method takes more simulation time and power than GA alternatives, at lower frequencies the computational power requirement are that of a home computer. More importantly, this method can realistically simulate sound wave phenomena simulated in reasonable time.

2.2 Wave-based Acoustic Simulation using the Finite-Difference Time-Domain Method

The fundamental value of the FDTD method is sound pressure. Sound pressure is the difference in air pressure relative to the steady-state atmospheric pressure, given by:

$$p_{sound} + p_{static} = p_{total} \quad (1)$$

Sound pressure can be expressed as a function of space (x , y and z) and time (t) as $p(x, y, z, t)$. Sound is a wave, moving at the speed of sound (c). The acoustic wave equation describes the fundamental relation between this speed, pressure, time, and space for sound as the following partial differential equation:

$$\frac{\partial^2 p}{\partial t^2} = c^2 \left(\frac{\partial^2 p}{\partial x^2} + \frac{\partial^2 p}{\partial y^2} + \frac{\partial^2 p}{\partial z^2} \right) \quad (2)$$

First, remember that the definition of a partial derivative is given by:

$$\frac{\partial f(x, y)}{\partial x} = \lim_{h \rightarrow 0} \frac{f(x + h, y) - f(x, y)}{h} \quad (3)$$

In reality, sound pressure is a continuous function. As h reaches zero, an infinite amount of x values have to be stored. This is impossible on a computer. For the purpose of simulation, an approximation with a certain degree of accuracy is desired. To address this issue, the finite difference method can be applied to the partial derivative. A finite difference describes the differential of a function at a position by approximating the slope using two know values and their relative spacing, with some error. This finite difference can be either forward ($f(x + h) - f(x)$), backwards ($f(x) - f(x - h)$) or central ($f(x + h) - f(x - h)$). The central finite difference operation is generally the most accurate. A central finite difference partial differential is given by:

$$\frac{\partial f(x, y)}{\partial x} \approx \frac{\delta_h[f](x, y)}{h} = \frac{f(x + h, y) - f(x - h, y)}{2h} \quad (4)$$

Note that this is *almost* equal to the actual differential. There is some error introduced. But, because the goal is to formulate an approximation, this will not be explicitly stated.

Another notation is to express the x coordinates as integer steps with spacing X . The notation becomes f_k where k is an integer number representing $k \cdot X = x$, and X replaces h as the spacing of values as such:

$$\frac{\partial f(x, y)}{\partial x} \approx \frac{\delta_X[f](x, y)}{X} = \frac{f_{k+1}^y - f_{k-1}^y}{2X} \quad (5)$$

in the second order form this becomes:

$$\frac{\partial^2 f(x, y)}{\partial x^2} \approx \frac{\delta_X^2[f](x, y)}{X^2} = \frac{f_{k+1}^y - 2f_k^y + f_{k-1}^y}{X^2} \quad (6)$$

This method can then be applied to Equation 2. First, we discretize the space described by the x , y and z -directions as an equally spaced grid with spacing X . Then T is introduced to denote the discretization of time. Using the notation introduced in Equation 5, the pressure function is discretized with respect to space (X) and time (T) as $p_{k,l,m}^n$ with $k \cdot X = x$, $l \cdot X = y$, $m \cdot X = z$ and $n \cdot T = t$. Applying a second order discrete central finite difference operator on the acoustic wave equation yields:

$$\frac{p_{k,l,m}^{n+1} - 2p_{k,l,m}^n + p_{k,l,m}^{n-1}}{T^2} = \frac{c^2}{X^2} (p_{k+1,l,m}^n - 2p_{k,l,m}^n + p_{k-1,l,m}^n + p_{k,l+1,m}^n - 2p_{k,l,m}^n + p_{k,l-1,m}^n + p_{k,l,m+1}^n - 2p_{k,l,m}^n + p_{k,l,m-1}^n) \quad (7)$$

The relation between c , T and X can be written as $\lambda = c \frac{T}{X}$. The value of λ is called the Courant number and its value should be ≤ 1 as a condition for the stability of the simulation[16].

Furthermore, the sum of spatial values is called a ‘‘stencil operation’’. We can express this as S , whose value is the sum of all six direct neighbouring cells in x , y and z - directions ($p_{l \pm 1, m \pm 1, i \pm 1}^n$). Equation 7 can then be rewritten as the following update equation:

$$p_{k,l,m}^{n+1} = \lambda^2 S + (2 - 6\lambda^2) p_{k,l,m}^n - p_{k,l,m}^{n-1} \quad (8)$$

To highlight the finite differences, Equation 8 can also be expressed as:

$$p_{k,l,m}^{n+1} = \lambda^2 (S - 3 \cdot 2p_{k,l,m}^n) + 2p_{k,l,m}^n - p_{k,l,m}^{n-1} \quad (9)$$

Note that there are different approaches to this approximation. A set of related approximations called compact explicit schemes is detailed in [8]. The main difference in these schemes is the different stencils they use. The one presented in Equation 8 is the rectilinear stencil and its scheme the Standard Leapfrog (SLF). This scheme is useful because it depends on the least amount of neighbours, while retaining good accuracy. Fewer look-ups results in increased performance, as detailed in Section 2.6. It is for that reason this scheme was utilized in this work.

2.3 Boundary Conditions

When sound hits a boundary, it does not flow unhindered through the boundary. Instead, the sound wave is reflected back with a fraction of its original power. This is the case for the outer limits of the simulated space, as well as solid objects inside. To handle this behaviour, a special update equation for the boundaries must be defined.

For the outer boundaries, one or more points in Equation 8 do not exist. These points are referred to as “ghost points” and have to be assigned a value. A simple solution is to set them to 0. This is equal to a grid point that ignores how the pressure around it changes.

As a result, sound waves are now reflected. However, the reflected waves have their phase inverted (i.e. upside down). Furthermore, they bounce without loss of energy, which is physically impossible. To remedy this, the simulation should correct for energy loss and phase preservation.

Realistically, boundaries lose energy based on the frequency of the signal. In other words, they are frequency dependant. Extensive methods have been devised to models these boundaries realistically [7], [17], often involving digital filters to account for frequency dependency.

However, these boundary conditions can be hard to implement. A simpler approach is to assume a frequency independent material, and inspect a range of frequencies. Moreover, the simulation is interested in a region of listener position (in the scale of thousands of cells). To get frequency domain information, all intermediate values have to be stored and converted with an Fourier Transform. This would result in a gigantic increase in memory use over time, and an increase in computing power to calculate each individual Fourier transform, even with a discrete fast Fourier transform. For the purpose of this simulation, only the response of the room to a signal of a fixed frequency is used. Therefore, this simulation can work with frequency independent boundary conditions.

To simulate energy absorbing boundaries, an absorption coefficient β must be defined which is the fraction of energy that the wave loses on a reflection. This coefficient is material dependant. Using the formulation described in [18], and representing the number of non-boundary (free air) neighbours as K the following update equation can be used for boundaries:

$$p_{k,l,m}^{n+1} = \frac{1}{1 + \lambda\beta} (\lambda^2 S + (2 - K\lambda^2)p_{k,l,m}^n - (1 - \lambda\beta)p_{k,l,m}^{n-1}) \quad (10)$$

in this equation, the variable K makes sure that the phase is corrected, while the new factors related to β ensure loss of energy. This equation can be used for both ghost points of the outer edges, as well as the ghost points of solid objects inside the space. Figure 1 illustrates the significant effect of boundary diffraction at lower frequencies, and how the wavefront correctly reflects while keeping phase and losing energy.

2.4 Source Excitation

To produce any meaningful results, a signal has to be “excited” (created) in the otherwise steady-state simulation space. The most straight forward approach to source excitation is the “hard” source[19]. This technique uses a special

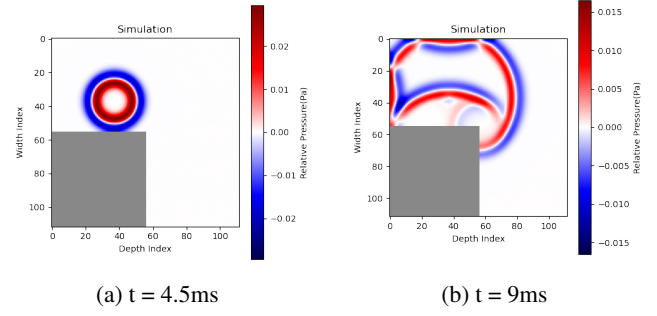


Figure 1: A wavefront of a 400hz signal reflecting and diffracting around a L-shaped room at two discrete time steps. The room in the picture is 6m in all dimensions. A significant amount of the wave is diffracted around the corner. Furthermore, the phase of the reflected wave is the same as the incoming wave, while losing some of its energy.

update function for a cell (grid point) at the source position, setting it to the value of the signal s :

$$p_{k,l,m}^{n+1} = s_{n+1} \quad (11)$$

Although the implementation of this technique is trivial, its effect on the simulation can be detrimental. Setting the signal directly result in the cell ignoring all normal simulation rules. This causes reflections and low-frequency scatterings in the simulation[19]. The result is unrealistic noise.

Another approach is the “soft” or “additive” source. In this approach, the signal is added into the simulation, with the source cells behaving just as any other cell. The update equation becomes:

$$p_{k,l,m}^{n+1} = \lambda^2 S + (2 - 6\lambda^2)p_{k,l,m}^n - p_{k,l,m}^{n-1} + s_{n+1} \quad (12)$$

A disadvantage of this method is that the sound pressure at the source location does not represent the actual input signal.

To improve source excitation, different approaches are possible[19], [20]. One option is the “transparent” source.

For a transparent source, the simulation is run to determine the effect of the room for that specific source location. This effect over time is stored and then subtracting from the excitation. This is more accurate, but also necessitates running two separate simulations. Moreover, it does not scale well with multiple source locations, requiring a separate calculation per source location.

Another option is to have a hybrid between a hard and soft source, where a hard source turns into a normal cell when the signal is done playing. However, this approach is only correct if the reflected waves do not reach the source location before it turns into a normal cell[21]. This condition is not the case if the goal is to inspect signal interference, for which the source must be turned on for a longer period.

Although it is the least realistic option, the hard source is used in this work. The reason being its simplicity and the accuracy of the signal. The simulation is fed with a simple sinusoidal signal. The soft source would distort the signal, thus diminishing the effect and accuracy of the room modes.

2.5 Measurement

After a signal is created in the simulated space, a measurement can be performed over the listener regions. In reality, an engineer would place one or more microphones at the location(s) of interest. In this simulation it is possible to measure *all* possible locations of interest at the same time, as the pressure value of every cell is calculated regardless.

Sound can be measured in a number of ways. A widely used measure is the sound pressure level (SPL), given by[22]:

$$L_p = 10 \log_{10} \left(\frac{p^2}{p_0^2} \right) \text{ dB} \quad (13)$$

where p is the simulated sound pressure and p_0 is the reference value given by $20 \mu\text{Pa}$ (the threshold of hearing)[22]. By taking the square of the sound pressure, it becomes a positive quantity that expresses the amplitude of the wave. This method does two things: it encapsulates the exponential nature of sound pressure, and its wave nature.

For the analysis, the property of interest is the energy transfer from a source to a listener cell over the whole simulated time. For that, the Equivalent Continuous Sound Level (often indicated by L_{eq}) is a useful metric. It describes a constant equivalent sound pressure level for a given signal over a time period t by:

$$L_{eq} = 10 \log_{10} \left(\frac{1}{t} \int_0^t \frac{p^2}{p_0^2} dt \right) \text{ dB} \quad (14)$$

For the simulation, a discrete variant of L_{eq} is used for position $p_{k,l,m}$:

$$L_{eq} = 10 \log_{10} \left(\frac{1}{t} \sum_{i=0}^t \frac{(p_{k,l,m}^i)^2}{p_0^2} T \right) \text{ dB} \quad (15)$$

2.6 GPU acceleration

A simulation step described by equations 8, 10 and 12 can be highly parallelized. That is the case because every cell is only relying on constant values to calculate a new value. As shown by multiple studies, significant performance gains (upt to 80 times) are achieved when the computation is done on the GPU, compared to the CPU[10], [15], [18], [23].

Two major factors influence the performance of a GPU “kernel” (program): the amount of overhead as compared to the number of computations, and the amount of look-ups in memory. The overhead consists mainly of moving data between the GPU and CPU memory. Look-ups should be minimized as they are a lot slower than computations on variables.

3 Method

3.1 Selecting Simulation Parameters

As defined in Section 2.2, the simulation is based on a discretized acoustic wave equation. The values of X and T largely influence the accuracy and stability of the simulation[16]. These values are highly dependant on the maximum frequency of interest (f_{max}) of the simulation.

To be able to measure a signal of frequency f_{max} , the grid spacing X must be at least equal to the minimal wavelength L :

$$X_{max} = L f_{max} = \frac{c}{f_{max}} \quad (16)$$

However, as noted by [8], a Standard Leapfrog scheme is only valid for frequencies below $0.196 f_{max}$. Therefore, a sampling frequency f_s must be used that compensates for this valid frequency range.

$$f_s > f_{max} \cdot 5.1 \quad (17)$$

For the simulation to be valid, the relation between T and X must conform to the maximum courant number for this simulation[8]. That is:

$$\lambda = \frac{1}{\sqrt{3}} = \frac{c \cdot T}{X}, \quad (18)$$

$$X = \frac{c}{f_s}, \quad T = \frac{1}{f_s \sqrt{3}}$$

Next to the resolution of the simulation, the resolution of the frequency space must be defined. Due to the exponential nature of frequencies, a linear scale is undesirable. Instead, acoustic measurements are done in octave bands. An octave band is a range of frequencies that span one octave. The definition of the k -th central frequency f_k for a $1/n$ -th fractional octave band around central f_0 is given by:

$$f_k = f_0 \cdot 2^{\frac{k}{n}} \quad (19)$$

As a standard, f_0 is set to 1000 hz[24]. When measuring over the full audible spectrum, measurements are usually done in $1/3$ fractional octave bands, but for the smaller sub-walker range a higher fraction is required for good results. High quality measurements are done in $1/24$ bands.

In the simulation, we will approximate the fractional octave bands in the 20 hz - 200 hz by their central frequency, as the simulation should not produce significant differences in material coefficients or response if the frequency resolution is large enough.

3.2 Virtually Representing a Room

To simulate a room, it first has to exist in the virtual space. The simulation expects an evenly spaced 3-D grid where each cell represents a cuboid region of the room. Previous work have used existing 3D models and converted triangles to their respective grid positions[15]. However, implementing (a tool for) the conversion of 3D models is outside the scope and time limits of this work. Instead, a grid is created given its outer dimensions, and rectangular cuboid regions can be marked as solid. The outer dimensions are assumed as solid. A solid region can be given a reflection (β) coefficient. The same applies for the six boundaries of the space, to be used in their respective “ghost points”.

Depending on the size of the grid spacing, some objects will be rounded off to their nearest grid position, or disappear entirely. The simulation therefore expects only objects that are large enough to have an influence on the acoustics of the room.

3.3 Running a GPU-Accelerated FDTD Simulation

Once a grid representation of the room has been defined, the next step is to run the simulation numerous times. As explained in Section 2.6 this simulation can benefit from a GPGPU implementation due to its parallel nature. This work uses an implementation in Python, but utilizes OpenCL[25] to perform the simulation steps.

To achieve the most performance, the data for the simulation is kept on the GPU as much as possible. To achieve this, the read-only data (boundaries, β values, geometry) are written once, and only the latest pressure and analytical values are written back to the CPU. The two previous pressure values are not synchronized between CPU and GPU. Furthermore, it is expected that a large number of consecutive iterations are performed by the GPU before returning the results to the CPU. To increase performance, a large amount of instructions are queued to the GPU.

For every iteration the following is queued: run a kernel that performs an iteration step for every cell; shift the pointers for the previous, current and next buffers in a round-robin fashion; run a kernel that calculates and stores the L_{eq} values based on the current pressure. Once the queue is empty, the newest pressure and analytical data is written back from the GPU buffer to the host buffer that the CPU can access.

A simulation with parameter f_s of 3200 hz ($200 \cdot 16$), and 136 million cells ($2000 m^3$), can simulate 10s of simulated time in 47 seconds in real time. This is equivalent to simulating around $400 m^3$ of simulated space per second at this frequency rate.

3.4 Measuring Frequency Response

With a virtual representation of the room, and a fast implementation, it can be used to obtain a frequency response for each possible subwoofer location. To get a response for a single frequency, the simulation must be run for an amount of time to allow the interference to develop and form a steady state L_{eq} . We call this time t_{sim} and it corresponds to a iteration number of:

$$i_{count} = \frac{t_{sim}}{T} \quad (20)$$

To get a full frequency response, a discrete set of frequencies is taken based on the central frequencies for 1/24 (or more) fractional octave bands within the 20 hz - 200 hz range. Then, for each frequency the simulation is run as described in the Section 3.3 for i_{count} iterations. When this is done, the average L_{eq} for all listener regions is stored and the simulation is reset. For every frequency, the β values are (re-)set based on a logarithmic interpolation of the material coefficients for 125hz and 250hz, and updated on the GPU. This process is repeated for every possible subwoofer location.

3.5 Locating the Optimal Source Location

Once the frequency response of each subwoofer location is known, an optimal location can be picked. Based on the frequency response, a source location can be assigned a qualitative metric. The metric used is the flatness, or minimal variance, of the response. In the optimal case, the response does not change over each frequency, i.e. the change in value

over each frequency is zero. This change in value is equal to the discrete derivative of the frequency response. To find the response with the least variation, we take the sum of square errors of the discrete derivative of the frequency response. The “error” in this case is the difference between the change in frequency response and its optimal value: zero. An error rating err can be expressed for the n values of L_{eq} for a single subwoofer location as:

$$err = \sum_{i=2}^n (L_i - L_{i-1})^2 \quad (21)$$

The optimal location should have the lowest value of err .

4 Results

4.1 Test setup

As a reference, a room was selected that could be modeled in the simulation as a reference. A picture of the selected room can be seen in Figure 2b. The inner dimensions of the room were measured to be 4.39m (width) by 3.32m (depth) by 2.69m (height). The far left corner (as seen from the entrance) was taken as grid axis origin. Next to the glass wall, a couch with a back rest is located. Two ottomans are located in the room: one below a TV at the far end wall, and one next to the right wall. Furthermore a small radiator is located next to the TV. The floor of the room is carpet, the three walls are hard walls, with the one covered in whiteboard, and the ceiling is a suspended ceiling system. A detailed floor plan of the room can be found in Appendix A.

The listener positions were indicated to be above the couch, the right ottoman and the middle of the room. The listening height was based on an estimate of ear positions for a sitting person: 1.0m - 1.4m. The listening height in the middle of the room was estimated as 1.6m - 2.0m.

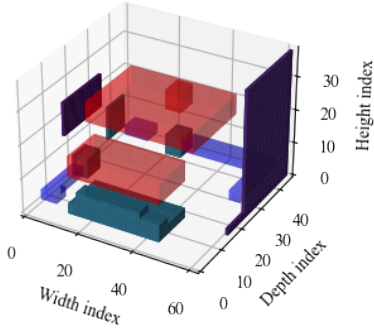
The subwoofers could realistically be placed on the floors outside of the walking routes and sitting areas. Furthermore, a subwoofer size was estimated as a cube of 40cm, which could at most be placed 20cm off the floor. Note that the center location of the source should coincide with the speaker. As such, a 20cm distance was taken from the floor and walls. A picture of the room, as well as its virtual representation can be viewed in Figure 2. Furthermore, Table 1 defines the reflection coefficients for the different materials in the room.

| ID | Material | 125hz | 250hz |
|----|-------------------|-------|-------|
| 1 | Carpet | 0.10 | 0.15 |
| 2 | Suspended ceiling | 0.15 | 0.11 |
| 3 | Hard wall | 0.04 | 0.05 |
| 4 | Double glass | 0.15 | 0.05 |
| 5 | Furniture | 0.32 | 0.40 |
| 6 | TV screen | 0.10 | 0.10 |
| 7 | Radiator | 0.35 | 0.39 |
| 8 | Wood | 0.10 | 0.07 |
| 9 | Whiteboard | 0.10 | 0.10 |

Table 1: Reflection coefficients used for the different materials in the reference room. These values are based on the ones found in [26] and [27] or estimated as 0.10.



(a) Reference room and test setup



(b) Virtual reference room

Figure 2: The reference room used in the experiment. (a) Is a picture of the room with the test setup and (b) its digital counterpart. In (b) the blue regions indicate a possible subwoofer location, while red regions mark all possible listening locations. The regions in purple and green are reflective objects in the room

4.2 Reference Measurements

To compare the simulation to its real life counterpart a measurement was made in the room using a Kien SUB subwoofer and a AKG C 417 PP omnidirectional microphone. The 44cm high subwoofer was placed in front of the TV screen with its center at 1.66m depth and 1.06m width. The microphone was hung on the whiteboard at 1.77m high, 18cm from the back wall and 3cm from the whiteboard. Using the tool Room EQ Wizard (REW) [28] a frequency response was measured.

Furthermore, REW has a built in room simulator. It uses a frequency domain adaption of the image source method described in [4] with additional absorption values for the boundaries. To show correlation to room modes, their frequencies can be highlighted. The value of a room mode f with index n_w, n_h, n_d corresponding to the width (w), height (h) and depth (d) of the room is defined by[1]:

$$f = \frac{c}{2} \sqrt{\left(\frac{n_w}{w}\right)^2 + \left(\frac{n_h}{h}\right)^2 + \left(\frac{n_d}{d}\right)^2} \quad (22)$$

The simulation was run for a f_s of 3200hz, for 1/48-th fractional octave bands and a t_{sim} per frequency of 5s with and without furniture. Figure 3 shows the difference in frequency response between measurement, simulation and an

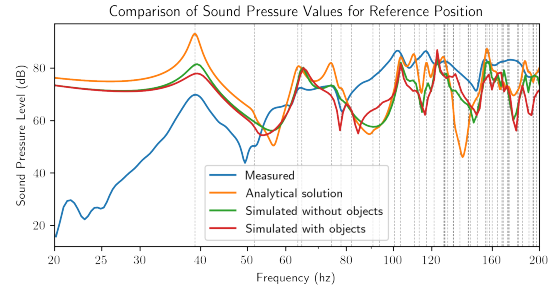


Figure 3: A comparison of the frequency response of the simulation, an analytical model for an empty room provided by [28], and a measured value. There is overlap in the influence of the room modes, which are highlighted by the vertical lines. The simulated response is less outspoken at the room mode frequencies than the analytical model. The subwoofer is rated for 30hz - 120hz.

alytical value compared to the outer room modes. There is a correlation between variations in frequency response and room mode frequencies. The measured response is relatively lower below 50 hz. The frequency response of the subwoofer was not calibrated for the measurement. It should be noted that the used subwoofer is rated for 30hz - 120hz.

When comparing the simulated response to the analytical model, there are some room mode frequencies excited differently, while overall showing correlation.

When comparing the simulated values with and without objects, the differences is that some resonant frequencies are relatively excited less while new resonant frequencies are introduced. At most, the difference is 14.6 dB, while on average the difference is 2.2 dB.

4.3 Influence of Simulated Time per Frequency

Furthermore, the effect of the t_{sim} was investigated. A higher value of t_{sim} is related to a longer time to reach a steady state. In Figure 4 the comparison is visible. A clear correlation between the variance at room mode frequencies can be observed for longer simulated time. Furthermore, at the shortest simulated time there is little correlation to room modes.

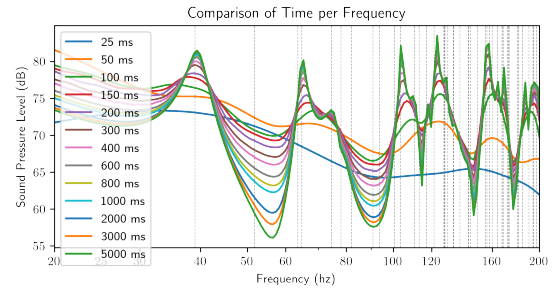


Figure 4: A comparison of the frequency response for different simulation time durations per frequency. On the vertical axis the resonant frequencies (room modes) for the outer boundaries are highlighted. A larger simulation time correlates to higher interference a room modes.

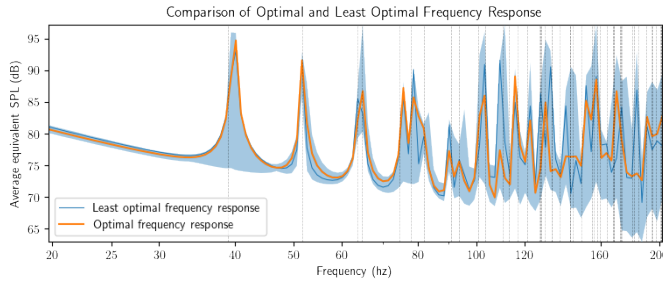


Figure 5: The frequency response with the most and the least variation (flatness) for the reference room. The blue region marks the minimum and maximum values for each frequency. As visible there is a significant difference in frequency response based on the location of the subwoofer. Furthermore, the optimal location has less variance in its response for some room modes, but not all room modes can be avoided. The room modes at 52 hz and 64 hz are unavoidable for all possible locations.

4.4 Frequency Response for All Locations

Next, a simulated optimization was run as described in Section 3.4 and 3.5. For the parameters, f_s was set to 200 hz with an oversampling factor of 16, and measured at 1/36-th fractional octave bands for 3s per frequency of interest. This last parameter was based on the results of Figure 4. For this grid spacing a total of 276 possible source locations were set. This simulation took around 17 hours to complete. For every source location the average frequency response was measured. The results can be viewed in Figure 5. There is a significant variation in frequency responses due to interference at resonant frequencies. For the possible locations in the scene, there is not one location that can avoid all resonances. Overall, the difference between the minimum and maximum L_{eq} for the most and least varying locations is nearly identical (24.8 dB and 24 dB).

4.5 Optimal location

The relative variation can be mapped to the spatial location of the subwoofer. This is shown in Figure 6. The flattest frequency response was found when placing the center of subwoofer at 0.27m in the width direction, at 27cm height and at 1.02m in the depth direction. In contrast, the least flat response was at 3.91m in the width direction, 27cm from the floor and 2.09cm in the depth direction.

5 Responsible Research

The research presented in this paper is a study of a mathematical model and a computer simulation. There are no human participants involved. This vastly decreases the possibility of unethical practises concerned with human harm. It does, however, not exclude indirect influences on human harm. Three factors for potential irresponsible research were identified. These are: reproducibility, validity of the results, and indirect harm.

An aim for this work was **reproducibility**. This was influenced by personal frustrations at the reproducibility of other papers. This is due to three causes: mathematical justifications that lacked information, unclear conversion of formulae

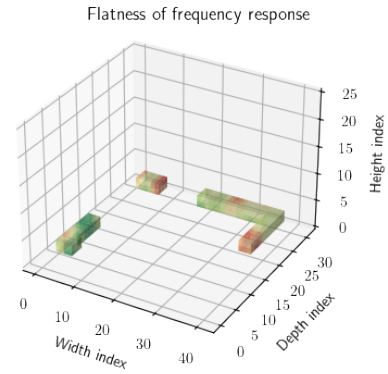


Figure 6: The relative variance of the frequency response for each source location on a scale from red (least optimal) to green (optimal). As visible, the best location is in the region at the 2nd width index and 9th depth index. This corresponds with the region left of the TV in the reference room.

to implementation, and provided code implementations that are platform locked.

This first cause can be attributed to personal lack of knowledge on this subject at the start of the research. Finite difference simulations, acoustics and GPGPU are not part of the common courses for a bachelor computer science engineer. This resulted in mathematical formulae lacking explanations of key concepts, expecting a different target audience. This paper attempts to clarify all necessary formulae in clear steps, to the degree they were understood themselves.

The second cause is a common occurrence when dealing with computer science papers. There is no standard for attributing an implementation in a paper. Moreover, the source code can not always be made opens source, due to reasons like copyright, intellectual property or contractual obligations. This paper tries to describe all steps necessary to reproduce the simulation, but provides the used implementation as open source¹.

The third cause can be attributed to the lack of standard for GPGPU frameworks and researchers producing code implementations in languages/frameworks that they are familiar with. The developed implementation in this research is based on two cross-platform technologies: Python and OpenCL. This combination can run on most platforms, as well as working on all modern GPU's (Nvidia, AMD) or devices that don't have a GPU. This makes it easier for researchers to run the code and reproduce the results or adopt the code. The source code also provides multiple real-time graphical interfaces so researchers can intuitively see how different parameters influence the simulation, some of which are used to generate the results.

Validity of the results is a recurring topic in responsible research. There is a bias towards positive results, resulting in a drive to skew results so they paint a pretty picture. The graphs provided in the results are all on the same scale, with points evenly spaced on each axis. All y-axis scales are automatically scaled to fit the data present. For all measurements

¹<https://github.com/delanoflipse/python-opencl-fdtd>

and simulations the parameters are given.

Indirect personal harm is not likely, but should not be overlooked. In case of a large discrepancy between simulated and real values, a user of the code might come to the wrong conclusion as to where the subwoofer should be placed. As mentioned, subwoofer placement can cause peaks in the frequency response. In a unlucky scenario, this might cause hearing damage if the listener is exposed to a higher volume sound.

6 Discussion and Future Work

The aim of this work was to investigate if a FDTD simulation can be utilized to find an optimal location for a subwoofer in a room. The results, in particular Figure 3, show that the room modes have a significant influence on the frequency response. This behaviour is present in both the simulated and the measured frequency response. A simulation of all possible locations and listener regions, as shown in Figure 2, showcases the significant effect of the location of the subwoofer on the frequency response. Using the frequency responses, an optimal subwoofer location was found within in the virtual room.

But, there are differences in both the analytic and simulated response, as well as the measured and simulated response.

The difference between the analytic and simulated response showcase a difference in how much interference each room mode creates. As shown by Figure 4, it takes time for the simulation to reach a steady state that fully resembles the room mode effect. This would explain some of the attenuated peaks. Furthermore, a finite difference scheme can not represent every sound reflection. Based on the angle of incidence, some reflections are not correctly simulated, as analyzed by [8] and [9]. Additionally, the boundary conditions do not simulate transmission, which at lower frequencies does play a role [2]. Overall, the simulation can benefit from more realistic boundary conditions.

Although the simulation accounts for some objects inside the simulated space, it only accounts for solid reflecting objects that are axis aligned. As analysed in [7], FDTD simulations are less accurate on rotated, or sloped objects. It should be noted that a Finite Volume approach can improve this, but makes the implementation harder, both in the virtualization of a room and in the update formulae.

To compare the results to an analytical solution, REW was used to generate a reference frequency response. REW is freeware but not open source. This means that, although a paper is stated on which the simulation is modeled, it is hard to pinpoint what exactly is the difference.

For the difference in measured response, a couple of factors play a role. The measurement was done using an uncalibrated microphone and subwoofer. This means that the results encompass both the room response, as wells as the behaviour of both devices. Furthermore, the subwoofer was rated for 30 hz - 120 hz². This is visible in Figure 3, where frequency response at below 50 hz are up to 40 dB lower. Interestingly, it is able to produce enough volume for frequency higher than its rating.

²As per the product specifications at <https://kien.io/>.

Import to note is that the simulation can only be as accurate as the accuracy of the simulated room. As highlighted in Table 1 the reflection coefficients are an estimation, based on a guess of both the material presents and even some material coefficients. To improve the measurements, and thus show an accurate difference between simulation and reality, a calibrated measurement should be performed, using a good microphone, a speaker with a sufficient range, and better investigated material coefficients. Previous work shows that this can result in a accurate correlation between measured and simulated [12].

The quality of the simulation also defines how well the “optimal” location is in reality. Currently, this optimization is based on the assumption that, if the frequency response is valid for one location, it is for all others. Due to time constraints it was not possible to perform a measurement of the “best” and “worst” location to verify their accuracy. Note that the simulated result encompasses 2200 listener positions and 276 possible source locations. To ensure the validity of the full simulation would require more than 600.000 measurements, which is unfeasible.

Another aspect that is not investigated is that, while an objective metric for a “better” location is used, there is a possibility that it does not translate well to how humans would perceive this as better. Using a different metric that has a psycho-acoustic basis might prove fruitful.

Moreover, it has been suggested by both [1] and [2] that multiple subwoofers can improve treating room modes. To add this to the optimization would amount to a quadratic growth in possible locations to check, even when filtering physically impossible combinations. And that is without accounting for possible optimization of phases. Without any “smart” reduction of the possible location, this would be unfeasible.

Overall, the presented method can be applicable to optimise subwoofer placement for the least variance in frequency response. There are clear paths to improving the accuracy of this method. Further work can investigate if the method can be extended to multiple subwoofers, and/or reduce the number of simulated subwoofer locations.

7 Conclusion

This paper investigated a method to optimize the placement of a subwoofer. It shows a proof of concept to minimize the variation in frequency response at a listener region. The Finite-Difference Time-Domain (FDTD) method was utilized to simulate sound through a virtual space. To validate the simulation, a physical measurement was performed in a room and compared to its virtual counterpart. The results show that the FDTD method can simulate sound with a correlation to both a measured frequency response and an analytical model.

All possible subwoofer locations in the virtual room were simulated, and an optimal location was found that provided the lowest variation in frequency response for all possible listening positions. However, the optimal location still contained variations in frequency response due to room mode resonances, but overall had less variation than other locations. Altogether, the method proves to be useful for rooms that

contain large objects or special geometry, for which a trivial solution is inaccurate.

References

- [1] T. Welti and A. Devantier, "Low-frequency optimization using multiple subwoofers," *J. Audio Eng. Soc.*, vol. 54, no. 5, pp. 347–364, May 2006.
- [2] F. E. Toole, *Sound Reproduction: Loudspeakers and Rooms*. Elsevier, 2008.
- [3] R. V. Waterhouse, "Output of a sound source in a reverberation chamber and other reflecting environments," *Journal of the Acoustical Society of America*, vol. 30, pp. 4–13, 1 1958, ISSN: NA. DOI: 10.1121/1.1909380.
- [4] J. B. Allen and D. A. Berkley, "Image method for efficiently simulating small-room acoustics," *Journal of the Acoustical Society of America*, vol. 65, pp. 943–950, 4 1979, ISSN: NA. DOI: 10.1121/1.382599.
- [5] A. R. Groh, "High-fidelity sound system equalization by analysis of standing waves," *journal of the audio engineering society*, vol. 22, no. 10, pp. 795–799, 1974.
- [6] D. Botteldoorena, "Finite-difference time-domain simulation of low-frequency room acoustic problems," *Journal of the Acoustical Society of America*, vol. 98, pp. 3302–3308, 6 1995, ISSN: NA. DOI: 10.1121/1.413817.
- [7] S. Bilbao, "Modeling of complex geometries and boundary conditions in finite difference/finite volume time domain room acoustics simulation," *IEEE Transactions on Audio, Speech and Language Processing*, vol. 21, pp. 1524–1533, 7 2013, ISSN: 15587916. DOI: 10.1109/TASL.2013.2256897.
- [8] K. Kowalczyk and M. V. Walstijn, "Room acoustics simulation using 3-d compact explicit ftd schemes," *IEEE Transactions on Audio, Speech and Language Processing*, vol. 19, pp. 34–46, 1 2011, ISSN: 15587916. DOI: 10.1109/TASL.2010.2045179.
- [9] J. Botts and L. Savioja, "Spectral and pseudospectral properties of finite difference models used in audio and room acoustics," *IEEE Transactions on Audio, Speech and Language Processing*, vol. 22, pp. 1403–1412, 9 Sep. 2014, ISSN: 15587916. DOI: 10.1109/TASLP.2014.2332045.
- [10] L. Savioja, "Real-time 3d finite-difference time-domain simulation of low- and mid-frequency room acoustics," Sep. 2010.
- [11] N. Morales and D. Manocha, "Optimizing source placement for noise minimization using hybrid acoustic simulation," *CAD Computer Aided Design*, vol. 96, pp. 1–12, Mar. 2018, ISSN: 00104485. DOI: 10.1016/j.cad.2017.09.007.
- [12] S. Sakamoto, H. Nagatomo, A. Ushiyama, and H. Tachibana, "Calculation of impulse responses and acoustic parameters in a hall by the finite-difference time-domain method," *Acoustical Science and Technology*, vol. 29, pp. 256–265, 4 2008, ISSN: 13463969. DOI: 10.1250/ast.29.256.
- [13] N. Tsingos, I. Carlbom, G. Elko, T. Funkhouser, and R. Kubli, "Validation of acoustical simulations in the "bell labs box"," *Computer Graphics and Applications, IEEE*, vol. 22, pp. 28–37, Aug. 2002.
- [14] S. Siltanen, T. Lokki, and L. Savioja, "Rays or waves? understanding the strengths and weaknesses of computational room acoustics modeling techniques," 2010.
- [15] M. Reuben, "Wayverb: A graphical tool for hybrid room acoustics simulation," 2017.
- [16] R Courant, K Friedrichs, and H Lewyt, "On the partial difference equations of mathematical physics."
- [17] K. Kowalczyk and M. V. Walstijn, "Formulation of locally reacting surfaces in ftd/k-dwm modelling of acoustic spaces," *Acta Acustica united with Acustica*, vol. 94, pp. 891–906, 6 Nov. 2008, ISSN: 16101928. DOI: 10.3813/AAA.918107.
- [18] C. J. Webb, "Parallel computation techniques for virtual acoustics and physical modelling synthesis," 2014.
- [19] D. T. Murphy, A. Southern, and L. Savioja, "Source excitation strategies for obtaining impulse responses in finite difference time domain room acoustics simulation," *Applied Acoustics*, vol. 82, pp. 6–14, 2014, ISSN: 0003682X. DOI: 10.1016/j.apacoust.2014.02.010.
- [20] J. B. Schneider, C. L. Wagner, and S. L. Broschat, "Implementation of transparent sources embedded in acoustic finite-difference time-domain grids," *The Journal of the Acoustical Society of America*, vol. 103, pp. 136–142, 1 Jan. 1998, ISSN: 0001-4966. DOI: 10.1121/1.421084.
- [21] H. Jeong and Y. W. Lam, "Source implementation to eliminate low-frequency artifacts in finite difference time domain room acoustic simulation," *The Journal of the Acoustical Society of America*, vol. 131, pp. 258–268, 1 Jan. 2012, ISSN: 0001-4966. DOI: 10.1121/1.3652886.
- [22] "Acoustics — Determination of sound power levels of noise sources — Guidelines for the use of basic standards," International Organization for Standardization, Tech. Rep. ISO 3740:2019, Feb. 2019.
- [23] M. Spindler, M. Masuch, and N. Röber, "Waveguide-based room acoustics through graphics hardware," 2006. [Online]. Available: <http://hdl.handle.net/2027/spo.bbp2372.2006.005>.
- [24] "Preferred Frequencies And Filter Band Center Frequencies For Acoustical Measurements," American National Standards Institute, Tech. Rep. ANSI/ASA S1.6-2016, Aug. 2016.
- [25] J. E. Stone, D. Gohara, and G. Shi, "Opencl: A parallel programming standard for heterogeneous computing systems," *Computing in Science and Engineering*, vol. 12, pp. 66–72, 3 May 2010, ISSN: 15219615. DOI: 10.1109/MCSE.2010.69.
- [26] [Online; accessed 18. Jan. 2023], May 2014. [Online]. Available: https://www.acoustic.ua/st/web_absorption_data_eng.pdf.

- [27] K. Studio, *Calcutta*, [Online; accessed 18. Jan. 2023], Jan. 2023. [Online]. Available: https://calcutta.com/sound_absorption_coefficients.
- [28] J. Mulcahy, *REW room acoustics and audio device measurement and analysis software*, [Online; accessed 28. Jan. 2023], Sep. 2022. [Online]. Available: <https://www.roomeqwizard.com>.

A Floor plan

The full measurement of the room is described in Figure A.1.

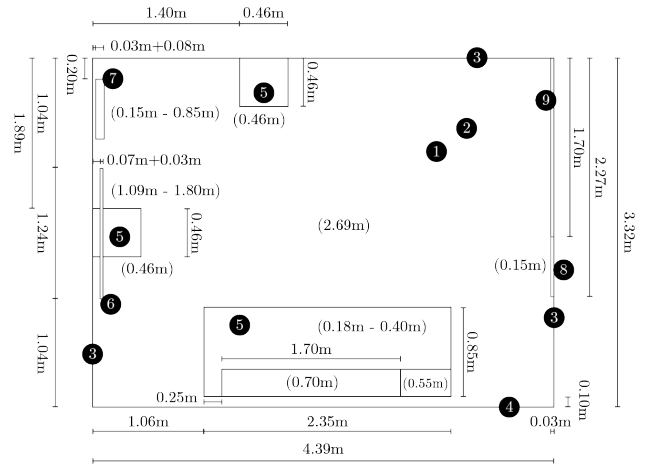


Figure A.1: The floor map of the simulated room used in the reference experiments. The circles denote a material, which corresponds to the values in Table 1.